HIV

Antibody-mediated prevention of vaginal HIV transmission is dictated by IgG subclass in humanized mice

Jacqueline M. Brady[1,2], Meredith Phelps[1,3], Scott W. MacDonald[1], Evan C. Lam[1], Adam Nitido[1,3], Dylan Parsons[1], Christine L. Boutros[1], Cailin E. Deal[1], Wilfredo F. Garcia-Beltran[1], Serah Tanno[1], Harini Natarajan[4], Margaret E. Ackerman[4,5], Vladimir D. Vrbanac[1], Alejandro B. Balazs[1]*

HIV broadly neutralizing antibodies (bNAbs) are capable of both blocking viral entry and driving innate immune responses against HIV-infected cells through their Fc region. Vaccination or productive infection results in a polyclonal mixture of class-switched immunoglobulin G (IgG) antibodies composed of four subclasses, each encoding distinct Fc regions that differentially engage innate immune functions. Despite evidence that innate immunity contributes to protection, the relative contribution of individual IgG subclasses is unknown. Here, we used vectored immunoprophylaxis in humanized mice to interrogate the efficacy of individual IgG subclasses during prevention of vaginal HIV transmission by VRC07, a potent CD4-binding site–directed bNAb. We find that VRC07 IgG2, which lacks Fc-mediated functionality, exhibited substantially reduced protection in vivo relative to other subclasses. Low concentrations of highly functional VRC07 IgG1 yielded substantial protection against vaginal challenge, suggesting that interventions capable of eliciting modest titers of functional IgG subclasses may provide meaningful benefit against infection.

INTRODUCTION

Broadly neutralizing antibodies (bNAbs) target conserved regions of the HIV envelope glycoprotein (Env) to inhibit infection through both direct neutralization of virus and recruitment of innate immunity to respond to HIV-infected cells. The Fc regions of antibodies engage Fc receptors on the surface of innate immune cells to elicit antibody-dependent cellular cytotoxicity (ADCC), phagocytosis (ADCP), and other effector functions. The immunoglobulin G (IgG) isotype comprises the majority of class-switched antibody produced in response to either vaccination or pathogen infection (*1*). However, IgG in humans is composed of four individual IgG subclasses (IgG1 to IgG4), each of which exhibits a unique pattern of binding to the numerous Fc gamma receptor (FcγR) proteins expressed by innate immune cells, yielding distinct capacities for each subclass to elicit effector functions (*2*).

The antibody-mediated prevention (AMP) study recently demonstrated that passive transfer of a CD4-binding site (CD4bs)–directed bNAb of the IgG1 subclass prevented transmission of sensitive strains to participants (*3*). Given the remarkable diversity of circulating strains, substantial effort is presently focused on the development of HIV vaccine regimens capable of eliciting bNAbs with maximal breadth and potency (*4*). However, existing vaccination regimens yield polyclonal antibody responses composed of all IgG subclasses (*5*), which may result in suboptimal protective efficacy. Although patients who naturally control their HIV infections have been shown to harbor a greater proportion of functional IgG subclasses (*6*), the efficacy of each individual subclass during prevention of HIV transmission has not been defined. Studies in both nonhuman primates (NHPs) using the simian immunodeficiency virus (SIV)–HIV chimeric virus (SHIV) and humanized mice using HIV have demonstrated that CD4bs-directed bNAbs of the IgG1 subclass exhibit reduced protection when harboring Fc mutations that limit effector functions (*7*, *8*). However, these findings have not held true for Fc variants of the V3-glycan–directed bNAb, PGT121, against either cell-associated or mucosal SHIV transmission in NHPs (*9*, *10*). Despite these conflicting results, recent studies in macaques have shown that passive transfer of highly functional IgGs correlates with improved protection against SIV transmission (*11*). However, these studies were conducted in simian models that do not entirely recapitulate human FcγR interactions (*12*). In addition, although previous studies have examined the relationship between in vitro bNAb potency and in vivo dose necessary to prevent transmission of chimeric SHIV in the NHP model (*13*–*15*), the precise relationship between bNAb concentration and risk of acquisition of transmitted founder HIV in the context of a human immune system has not been established. The minimum protective dose of IgG bNAbs and the effector cell activities that coordinate with distinct human IgG subclasses to prevent HIV transmission remain unknown, despite their critical importance to the success of ongoing efforts to develop vaccines and prophylactic interventions. A central issue has been that most animal models do not permit an examination of HIV infection in the context of a human immune response.

In this study, we used humanized mice, which harbor human innate immune cells bearing the full complement of FcγRs, to determine the relative potential of each IgG subclass to prevent infection by a transmitted founder strain of HIV. For antibody delivery, we and others have described vectored immunoprophylaxis (VIP), using adeno-associated virus (AAV) vectors to deliver transgenes encoding antibodies to muscle tissue, resulting in long-term, systemic production of bNAbs capable of protecting humanized mice

[1]Ragon Institute of Massachusetts General Hospital, Massachusetts Institute of Technology and Harvard University, Cambridge, MA 02139, USA. [2]Department of Biological and Biomedical Sciences, Harvard Medical School, Boston, MA 02115, USA. [3]Department of Virology, Harvard Medical School, Boston, MA 02115, USA. [4]Department of Microbiology and Immunology, Geisel School of Medicine at Dartmouth, Dartmouth College, Hanover, NH 03755, USA. [5]Thayer School of Engineering, Dartmouth College, Hanover, NH 03755, USA.
*Corresponding author. Email: abalazs@mgh.harvard.edu

and NHPs from HIV, SHIV, or SIV challenge (*16*–*19*). This dose-dependent expression of genetically encoded bNAb enabled dissection of the precise contribution of each IgG subclass in vivo. Using this approach, our study defined the individual contributions of IgG subclasses during prevention of vaginal HIV transmission. Our findings suggest that subclasses with diminished capacity to mediate both ADCP and ADCC exhibit reduced protection as compared to more functional IgG subclasses but only at low circulating antibody concentrations. This is particularly relevant to bNAb elicitation by vaccination, where antibody concentrations are also expected to be low. Analysis of the relative efficacy of protection across a range of IgG1 doses yielded a statistical model of the relationship between bNAb concentration and risk of infection, demonstrating that even modest concentrations of functional antibodies can prevent transmission.

RESULTS

VRC07 IgG subclasses exhibited distinct effector function activity in vitro

To produce antibodies with different Fc functionality, we generated AAV serotype 8 expression vectors encoding the VRC07 variable region followed by the constant region of each human IgG subclass: IgG1, IgG2, IgG3, and IgG4 (fig. S1A and table S1). Heavy and light chains were expressed from a single transgene separated by a furin-2A picornavirus self-processing peptide as has been previously described (*16*). As anticipated, Fc modulation of VRC07 had minimal impact on the ability of purified proteins (fig. S1B) to neutralize HIV in vitro (Fig. 1A) or bind to HIV-1 Env expressed on the surface of cells (Fig. 1B and fig. S2A). However, Fc alteration did affect binding of FcγRs to VRC07-bound target cells as measured by flow cytometry (fig. S2, B and C). FcγRs bound to VRC07 IgG1 and IgG3 at lower half-maximal binding concentrations (EC_{50}) than the other VRC07 IgG subclasses, indicating a higher affinity binding interaction between these IgG subclasses and FcγRs (Fig. 1C and fig. S2D). Although IgG4 demonstrated comparable binding to FcγR1a, it had markedly reduced binding to all other FcγRs tested. Nearly all FcγRs exhibited poor binding to IgG2, consistent with previous reports for other specificities (*20*).

To determine whether FcγR binding differences affected Fc function, we measured the ability of VRC07 IgG subclasses to mediate ADCP and ADCC activity in cell-based effector function assays. We began by measuring the ability of these antibodies to induce THP-1 cells to engulf CEM.NKr target cells, stably expressing $HIV_{JR\text{-}CSF}$ Env and a ZsGreen fluorescent reporter protein (Fig. 1D and fig. S3A). In this assay, IgG1 and IgG3 showed equivalent ability to facilitate phagocytosis by THP-1 effector cells. IgG4 led to reduced phagocytic activity compared to IgG1 but still maintained

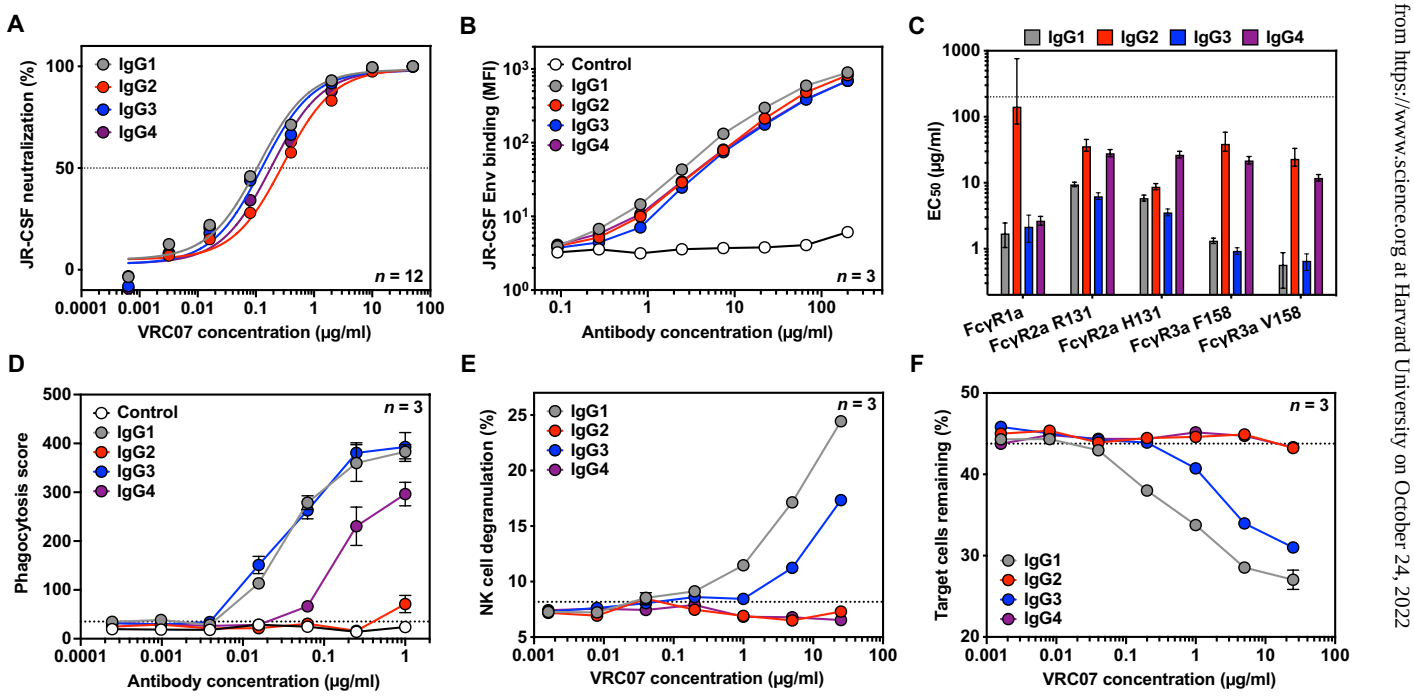

Fig. 1. IgG subclass switching affects the ability of VRC07 to bind FcγRs and mediate effector function activity. (**A**) In vitro neutralization activity of purified VRC07 IgG subclasses against $HIV_{JR\text{-}CSF}$ was measured by TZM-bl neutralization assays ($n = 12$ per group). The horizontal dotted line indicates 50% neutralization activity. Error bars represent SEM. (**B**) Binding of VRC07 IgG subclasses or a malaria-specific negative control IgG1 antibody to $HIV_{JR\text{-}CSF}$ Env-expressing target cells was measured by flow cytometry with a pan-IgG-Fc detection reagent ($n = 3$ per group). Error bars represent SEM. (**C**) Half-maximal binding concentrations (EC_{50}) of cell surface-bound VRC07 IgG subclasses to purified fluorescent-labeled FcγR proteins were measured by flow cytometry. The dotted line represents the maximum concentration tested. Error bars denote the 95% confidence interval. (**D**) Phagocytosis of $HIV_{JR\text{-}CSF}$ Env-expressing target cells by THP-1 cells mediated by VRC07 IgG subclasses or a malaria-specific negative control IgG1 antibody was measured by flow cytometry ($n = 3$ per group). The dotted line indicates the average phagocytic score in the absence of a VRC07 antibody. Error bars represent SEM. (**E** and **F**) The ability of VRC07 IgG subclasses to mediate NK cell degranulation (E) or specific killing of $HIV_{JR\text{-}CSF}$ Env-expressing target cells (F) was measured by flow cytometry ($n = 3$ per group). Results are from a representative NK cell donor. The dotted lines indicate the average value in the absence of a VRC07 antibody. Error bars represent SEM.

some activity at higher concentrations. IgG2, on the other hand, was unable to mediate any phagocytic activity over background. To confirm these findings, we used an antigen-coated bead-based phagocytosis assay with multiple HIV Env variants as previously described (fig. S3, B to D) (*21*). IgG3 mediated considerably more potent phagocytosis of HIV gp120-coated beads than either IgG1 or IgG4, as has been previously observed for other HIV-specific monoclonal antibodies (*22*, *23*). IgG2, however, mediated little to no phagocytic activity of beads over background even at the highest concentration tested.

To measure ADCC, we performed analogous cell-based killing assays using $HIV_{JR\text{-}CSF}$ Env-expressing cells mixed with nontransduced, parental CEM.NKr cells. Incubation of the mixed target population with antibody and donor-derived natural killer (NK) cells led to a considerable increase in degranulation of NK cells, which corresponded with specific depletion of Env-expressing target cells from the population. Although this observation held true for IgG1 and IgG3 antibodies, neither IgG2 nor IgG4 antibodies were able to induce NK cell degranulation or target cell killing. Even at the highest concentration tested, these antibodies were indistinguishable from the control in which no antibody was added (Fig. 1, E and F, and fig. S4A). To confirm these findings, assays were repeated with NK cells isolated from a genetically distinct donor (fig. S4, B and C). Together, these assays demonstrated that changes to VRC07 IgG subclass had minimal impact on neutralization and epitope binding but altered the capacity of VRC07 to mediate Fc effector function activity, with IgG1 and IgG3 mediating both ADCC and ADCP, IgG4 mediating ADCP but no ADCC, and IgG2 mediating neither innate function.

High plasma concentrations of VRC07 prevented HIV acquisition in a simplified humanized mouse model regardless of IgG subclass

We next confirmed the in vivo efficacy of the VRC07 IgG subclasses when delivered by VIP. To this end, we performed an HIV challenge study in human peripheral blood mononuclear cell (huPBMC)–engrafted nonobese diabetic (NOD)/severe combined immunodeficient (SCID)/$\gamma c^{-/-}$ (NSG) mice (huPBMC-NSG) using the established conditions and $HIV_{NL4\text{-}3}$ strain that we previously described (Fig. 2A) (*16*). This simplified humanized mouse model is predominantly engrafted with $CD3^+$ T cells with little to no NK or myeloid cell functionality (*24*, *25*). Therefore, antibody-mediated HIV protection studies in huPBMC-NSG mice are highly dependent on neutralization. The VRC07 IgG subclasses exhibited no difference in neutralizing activity against $HIV_{NL4\text{-}3}$, in vitro (Fig. 2B). To achieve in vivo expression of VRC07 IgG subclasses, we performed intramuscular injections of AAV encoding each antibody construct or firefly luciferase as a negative control. Eight weeks after intramuscular AAV administration, mice achieved average plasma concentrations ranging from 50 to 80 μg/ml for VRC07 IgG1, IgG2, and IgG4 (Fig. 2C). Mice expressing VRC07 IgG3 achieved plasma concentrations of about 10 μg/ml, which was substantially above the 5 μg/ml previously shown to be the minimum protective dose for VRC07 IgG1 against $HIV_{NL4\text{-}3}$ in this model (*17*). After 8 weeks of expression, the NSG mice were humanized by injection of activated huPBMCs and, 2 weeks later, were challenged with a single intravenous administration of $HIV_{NL4\text{-}3}$ (Fig. 2A). HIV infection was assessed by weekly quantitation of both $CD4^+$ T cell depletion and viral load in peripheral blood (Fig. 2D). Seven of the nine control mice that received AAV-luciferase became infected after challenge, whereas all mice that received AAV-VRC07, regardless of the IgG subclass, were completely protected (Fig. 2E). These results demonstrate that all four IgG subclasses are capable of mediating protection in vivo when present at high plasma concentration in a simplified humanized mouse model.

VRC07 Fc variants elicited distinct functional profiles against transmitted founder HIV

As most HIV infections occur through sexual transmission, we sought to investigate the impact of IgG subclass on VRC07-mediated protection from vaginal HIV challenge. To model an HIV variant capable of transmitting between humans, we used $HIV_{REJO.c}$, a transmitted molecular founder strain (*26*). IgG subclass did not affect the in vitro neutralizing activity of VRC07 against $HIV_{REJO.c}$ (Fig. 3A). In addition, we tested a VRC07 IgG1 variant harboring two leucine-to-alanine substitutions at positions 234 and 235 (VRC07 LALA) as these mutations have previously been used to assess the contribution of effector function to bNAb-mediated protection (*7*–*10*). Compared to VRC07 IgG1, the LALA variant retained in vitro neutralization activity but exhibited reduced binding to human FcγRs as previously described (Fig. 3A and fig. S5) (*27*).

To assess the functionality of the VRC07 Fc variants against $HIV_{REJO.c}$, we performed the aforementioned cell-based binding, ADCP, and ADCC assays with $HIV_{REJO.c}$ Env-expressing cells in the target population (Fig. 3, B to E). All VRC07 Fc variants displayed equivalent binding of cell surface $HIV_{REJO.c}$ Env (Fig. 3B). VRC07 IgG1, IgG3, IgG4, and LALA exhibited comparable ability to mediate phagocytosis by THP-1 effector cells. IgG2 also facilitated detectable phagocytic activity at higher concentrations, although it was substantially lower than that observed for the other Fc variants (Fig. 3C). When ADCC assays were performed with $HIV_{REJO.c}$ Env-expressing cells, VRC07 IgG1 and IgG3 mediated a considerable increase in degranulation of NK cells that corresponded with specific depletion of Env-expressing target cells from the population. However, VRC07 IgG2, IgG4, and LALA were unable to mediate NK cell degranulation or target cell killing, similar to results seen for $HIV_{JR\text{-}CSF}$ (Fig. 3, D and E).

VRC07 Fc variants exhibited differential protective efficacy against vaginal HIV transmission in humanized mice

We investigated the in vivo efficacy of each VRC07 IgG subclass against vaginal transmission of the transmitted founder strain, $HIV_{REJO.c}$, using the bone marrow–liver-thymus (BLT) humanized mouse model. This model consists of surgically implanted human thymic tissue and transplantation of genetically matched $CD34^+$ hematopoietic stem cells, resulting in extensive multilineage engraftment of human immune cells throughout the animal, which render it susceptible to vaginal or rectal challenge (Fig. 4A) (*17*, *28*–*30*). To determine the potential for human cells in BLT mice to participate in innate immune interactions with human anti-HIV antibodies, we first characterized the relative frequency of innate immune cell types in peripheral blood. We noted that BLT mice harbored T cells, B cells, and myeloid cells at frequencies similar to those found in human blood (*31*), whereas NK cells were present at lower frequencies (Fig. 4B). Flow cytometric analysis of immune cells in the peripheral blood of uninfected BLT humanized mice revealed that NK and myeloid cell subsets expressed the expected pattern of human FcγRs (Fig. 4C and fig. S6). Specifically, a substantial percentage of circulating NK cells expressed FcγR3 (CD16), the receptor involved in mediating ADCC. Furthermore, a large proportion of the myeloid

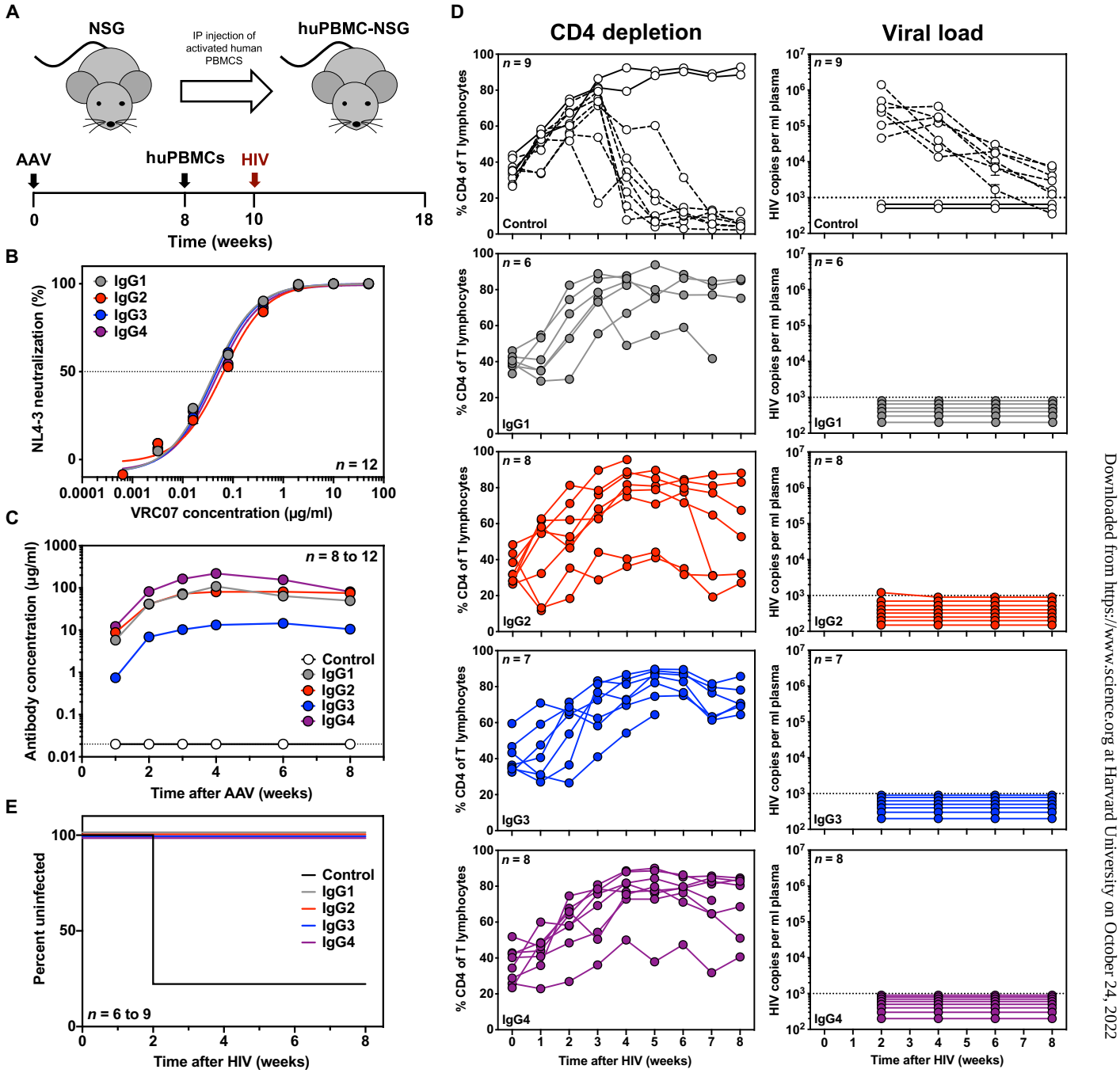

Fig. 2. IgG subclass switching does not affect the ability of VRC07 to protect from HIV challenge in huPBMC-NSG mice. (**A**) Overview of the huPBMC-NSG mouse model with a schematic representation of the experimental timeline. IP, intraperitoneal. (**B**) In vitro neutralization activity of purified VRC07 IgG subclasses against the challenge strain, HIV_{NL4-3}, was measured by a TZM-bl neutralization assay ($n = 12$ per group). The horizontal dotted line indicates 50% neutralization activity. Error bars represent SEM. (**C**) Average plasma antibody concentrations achieved in NSG mice were measured by ELISA after intramuscular injection of 2.5×10^{11} genome copies (GC) of AAV expressing a given VRC07 IgG subclass or firefly luciferase (control) as a negative control ($n = 8$ to 12 mice per group). Error bars represent SEM. The horizontal dotted line indicates the limit of detection, 0.02 μg/ml, for the assay. (**D**) CD4 T cell depletion (left) and viral load (right) were measured in the peripheral blood of huPBMC-NSG mice expressing luciferase (control) or a VRC07 IgG subclass after intravenous challenge of 280 TCID50 HIV_{NL4-3}. Viral load was measured by qPCR. The dotted lines indicate the limit of detection, 1000 copies/ml. Samples with undetectable viral load were assigned an arbitrary value below the limit of detection. CD4 depletion was measured by flow cytometry. The dashed lines indicate mice that were confirmed to be infected by qPCR. (**E**) Kaplan-Meier survival curves for huPBMC-NSG mice expressing the given VRC07 IgG subclass or negative control. Survival curves of all VRC07 IgG subclasses were significantly different as compared to control ($P < 0.0001$) by log-rank (Mantel-Cox) test.

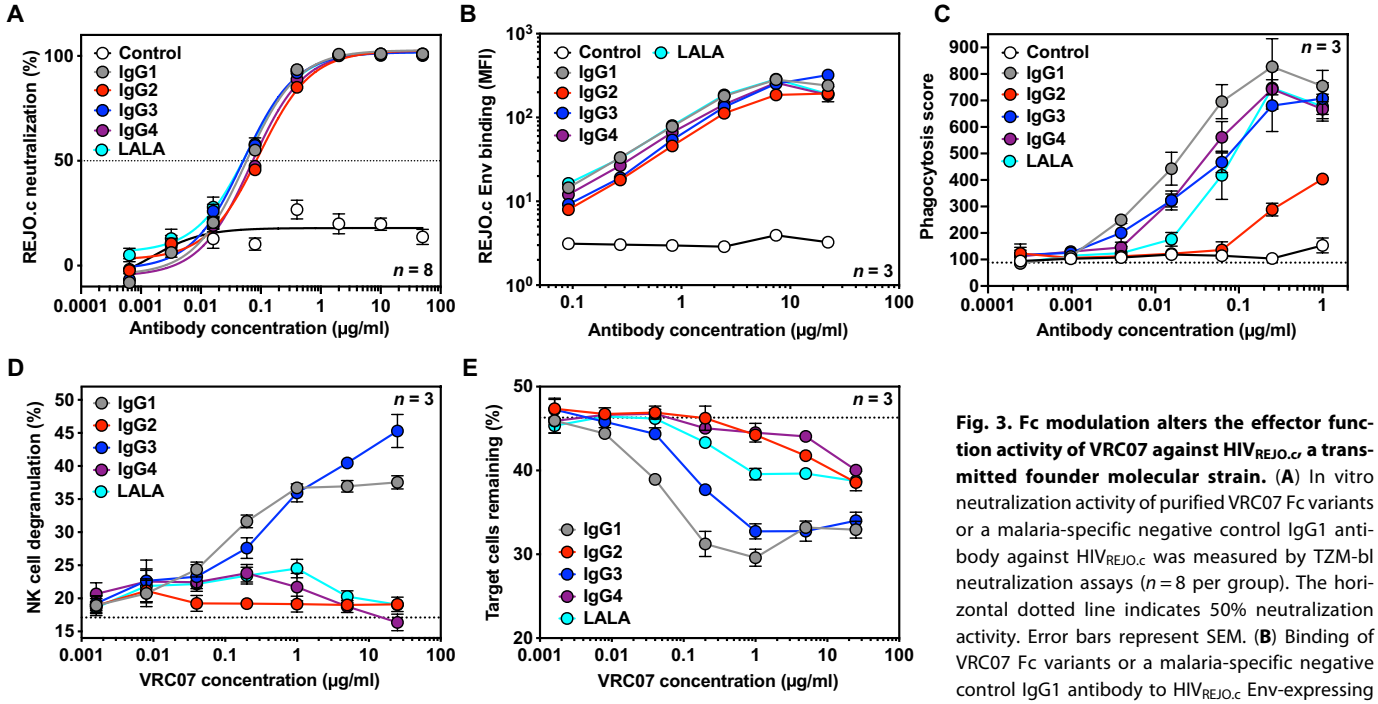

Fig. 3. Fc modulation alters the effector function activity of VRC07 against $HIV_{REJO.c}$, a transmitted founder molecular strain. (**A**) In vitro neutralization activity of purified VRC07 Fc variants or a malaria-specific negative control IgG1 antibody against $HIV_{REJO.c}$ was measured by TZM-bl neutralization assays ($n = 8$ per group). The horizontal dotted line indicates 50% neutralization activity. Error bars represent SEM. (**B**) Binding of VRC07 Fc variants or a malaria-specific negative control IgG1 antibody to $HIV_{REJO.c}$ Env-expressing target cells was measured by flow cytometry with a pan-IgG-Fc detection reagent ($n = 3$ per group). Error bars represent SEM. (**C**) Phagocytosis of $HIV_{REJO.c}$ Env-expressing target cells by THP-1 cells mediated by VRC07 Fc variants or a malaria-specific negative control IgG1 antibody was measured by flow cytometry ($n = 3$ per group). The dotted line indicates the average phagocytic score in the absence of a VRC07 antibody. Error bars represent SEM. (**D** and **E**) The ability of VRC07 Fc variants to mediate NK cell degranulation (D) or specific killing of $HIV_{REJO.c}$ Env-expressing target cells (E) was measured by flow cytometry ($n = 3$ per group). Results are from a representative NK cell donor. The dotted lines indicate the average value in the absence of a VRC07 antibody. Error bars represent SEM.

cell subset, which included monocytes and dendritic cells (DCs), also expressed FcγR3 in addition to FcγR2 (CD32) and FcγR1 (CD64) that are involved in mediating ADCP.

To determine the potential of FcγR-expressing cells in BLT mice to interact with the four subclasses of VRC07, we performed additional flow cytometry using fluorescently labeled VRC07 IgG1 to IgG4 proteins, as well as VRC07 LALA. Exposure of splenocytes harvested from BLT mice to fluorescently labeled VRC07 proteins revealed that monocytes interacted most strongly with IgG1 and IgG3. IgG4 exhibited modest staining, whereas IgG2 and LALA resulted in limited interaction with monocytes (Fig. 4D and fig. S7). NK cells in the spleen did not interact appreciably with labeled VRC07 in this experiment; however, we observed a similar lack of NK cell staining in one of two healthy human donors, suggesting that human immune cells in BLT mice display similar patterns of interactions with IgG subclasses as immune cells in humans (fig. S7).

To determine the relative protective efficacy of each IgG subclass against repetitive challenge with HIV, we administered AAV expressing each VRC07 subclass (IgG1, IgG2, IgG3, IgG4, or LALA) to BLT mice at different doses to achieve plasma antibody concentrations ranging from 70 μg/ml to less than 0.05 μg/ml (Fig. 4E and fig. S8). In addition, as a negative control, we compared these to BLT mice expressing high concentrations of 2A10, an irrelevant malaria-specific human IgG1 antibody (*32*). Five weeks after AAV administration, we initiated weekly vaginal challenges of $HIV_{REJO.c}$ for 15 consecutive weeks, and measured the rate of infection by plasma viral load (fig. S9). To ensure reproducibility of the observed results and control for variable immune reconstitution, we combined results from three separate experiments performed with distinct batches of BLT mice (table S1).

Across 29 mice expressing the negative control antibody, we detected plasma antibody concentrations ranging from roughly 1 to 250 μg/ml (Fig. 4E and fig. S8). All but one of these mice, regardless of circulating antibody concentration, became infected after three repeated vaginal challenges with HIV. The remaining control mouse became infected after nine challenges (Fig. 4F). All VRC07 Fc variants conferred measurable protection against HIV acquisition when compared to the negative control antibody (Fig. 4F). VRC07 IgG3, IgG4, and LALA did not exhibit different in vivo efficacy as compared to IgG1 (Fig. 4F). Overall, VRC07 IgG3 achieved lower plasma antibody concentrations than the other Fc variants, with three mice expressing less than 1.5 μg/ml, exhibiting no protection, and four mice expressing more than 4 μg/ml, exhibiting either delayed acquisition or complete protection. Mice expressing VRC07 IgG4 exhibited a wide range of antibody concentrations from less than 1 μg/ml to more than 70 μg/ml. Eight of 10 animals expressing VRC07 IgG4 of less than 1 μg/ml exhibited no protection, whereas 3 of 12 mice expressing VRC07 IgG4 of more than 5 μg/ml delayed acquisition; the rest exhibited complete resistance. Mice expressing VRC07 LALA followed the same trend, with three of four mice harboring less than 3 μg/ml in circulation, exhibiting no protection; in contrast, 7 of 18 mice above 6 μg/ml showed a substantial delay in HIV acquisition with those above 10 μg/ml completely protected. All of these IgG subclasses, including IgG1-LALA, retained substantial phagocytic activity in vitro, particularly against cells expressing Env from the challenge strain, $HIV_{REJO.c}$, used in this experiment (Fig. 3B).

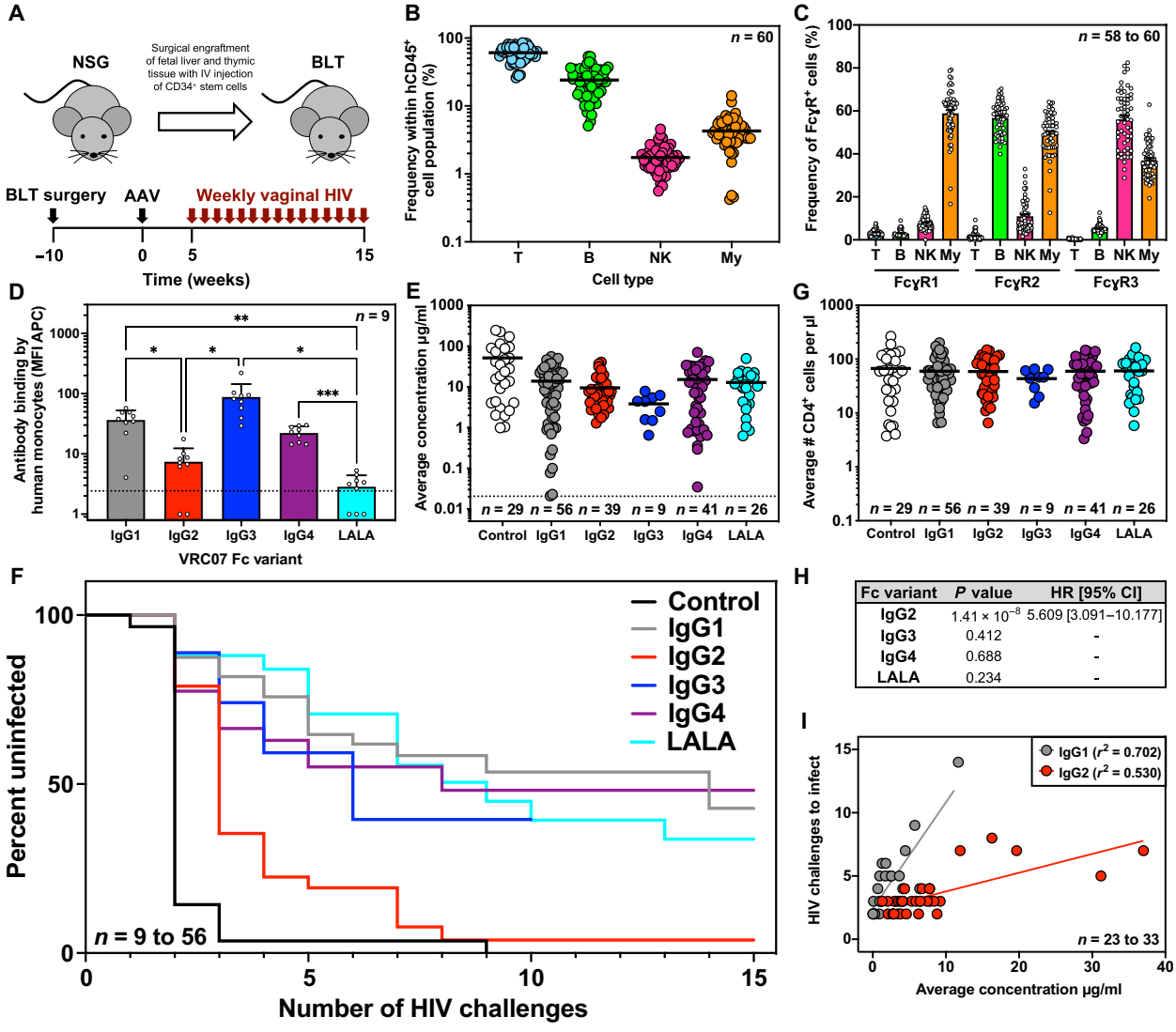

Fig. 4. VRC07 Fc variants exhibit distinct protective efficacy against repetitive HIV vaginal challenge in BLT humanized mice. (**A**) Overview of BLT humanized mouse model and schematic representation of experimental timeline. IV, intravenous. (**B**) The frequency of human T cells ($CD45^+$ and $CD3^+$), B cells ($CD45^+$ and $CD19^+$), NK cells ($CD45^+$, $CD3^-$, $CD19^-$, and HLA-DR^-, $CD56^+$), and myeloid cells (My; $CD45^+$, $CD3^-$, $CD19^-$, $CD11c^+$, and HLA-DR^+) in the peripheral blood of uninfected BLT mice ($n = 60$) were measured at 10 weeks after surgical engraftment by flow cytometry. Horizontal bars represent the mean. (**C**) The percentages of the human immune cell subsets from (B) expressing human FcγR1, FcγR2, or FcγR3 were measured by flow cytometry. Bars represent the mean; error bars represent SEM. (**D**) Binding of AF647-labeled VRC07 Fc variants by human monocytes ($CD45^+$, $CD3^-$, $CD56^-$, and $CD14^+$) isolated from the spleens of BLT mice ($n = 9$) was measured across two separate BLT batches by flow cytometry. The dotted line indicates the average MFI in the absence of a VRC07 antibody. Bars represent the mean and SD with statistical significance determined by one-way analysis of variance with Tukey's correction for multiple comparisons. $^*P < 0.02$, $^{**}P < 0.01$, and $^{***}P < 0.001$. (**E**) Average plasma antibody concentrations achieved in BLT mice from the start of vaginal challenges through HIV acquisition or death were measured. Mice were given 1.0×10^{10} to 2.5×10^{11} GC of AAV expressing the given VRC07 Fc variant or a malaria-specific negative control IgG1 antibody, and plasma concentrations were measured weekly by gp120 or malaria-specific ELISA. Graphs represent combined data from three separate BLT experiments with the exception of VRC07 IgG3 (one experiment) and VRC07 LALA (two experiments). Horizontal bars indicate the mean. The dotted line indicates the limit of detection, 0.02 µg/ml, for the assay. (**F**) Kaplan-Meier survival curves are shown for mice expressing VRC07 Fc variants or a malaria-specific negative control IgG1 antibody after repeated intravaginal HIV challenge. (**G**) Average numbers of human $CD4^+$ cells per microliter of blood in BLT mice from the start of vaginal challenges through HIV acquisition or death were measured by flow cytometry. Horizontal bars indicate the mean. (**H**) Cox regression analysis of the effect of Fc modulation on the rate of HIV acquisition across multiple BLT experiments controlled for antibody concentration is shown. A hazard ratio (HR) and 95% confidence interval (CI) are only reported if the *P* value was less than 0.05. (**I**) The relationship between the average circulating antibody concentration (micrograms per milliliter) and the number of HIV challenges required for infection to occur over the course of challenge in BLT humanized mice was plotted. Lines represent the result of a linear regression for mice expressing VRC07 IgG1 ($n = 23$ mice) or VRC07 IgG2 ($n = 33$ mice).

In contrast, VRC07 IgG2 showed a marked reduction in protective efficacy when compared to IgG1. Despite average plasma IgG2 concentrations between 1.2 and 9.2 µg/ml, 28 mice became infected within four challenges, whereas nearly all others were infected within eight challenges. The only mouse to achieve complete protection from 15 repeated vaginal challenges expressed an average circulating VRC07 IgG2 concentration over 40 µg/ml. The observed differences in HIV acquisition are likely not the result of differential

T cell engraftment, as mice in each group had comparable $CD4^+$ cell numbers in peripheral blood over the course of the experiment (Fig. 4G and fig. S10).

When all Fc variants were compared to IgG1 using a Cox regression analysis, we found a statistically significant association ($P = 1.41 \times 10^{-8}$) between IgG2 and the rate of HIV acquisition (Fig. 4H). The associated hazard ratio indicates that mice expressing VRC07 IgG2 had greater than 5.6-fold increased risk of HIV infection compared to mice expressing VRC07 IgG1, irrespective of antibody concentration. When directly comparing VRC07 IgG2-expressing mice to VRC07 IgG1-expressing mice that became infected over the course of the study, the correlation between antibody concentration and the number of challenges required to infect was distinct (Fig. 4I). These results demonstrate that substantially more IgG2 antibody is required to achieve the same reduction in risk provided by IgG1.

Modest plasma concentrations of VRC07 IgG1 protected against vaginal HIV challenge in humanized mice

Given the extensive clinical use of IgG1 subclass antibodies in human passive transfer studies, we sought to better define the concentration-dependent protective efficacy of this subclass. Our laboratory has previously shown that the G54W variant of VRC07 IgG1 can fully protect BLT mice from repeated challenges of the transmitted founder strain, $HIV_{REJO.c}$, when present at about 100 μg/ml in plasma (*17*). To determine the minimum protective concentration of VRC07 IgG1, we reanalyzed HIV acquisition in the aforementioned BLT challenge studies (table S2) across a wide range of concentrations (Fig. 5A). Specifically, mice receiving AAV-VRC07-IgG1 were grouped on the basis of average weekly plasma antibody concentration over the course of HIV challenge (fig. S8). This metric was used to categorize mice into high (greater than 12 μg/ml), medium (2 to 12 μg/ml), or low (less than 2 μg/ml) expression groups.

All 25 mice in the high expression group were completely protected from 15 consecutive vaginal challenges with $HIV_{REJO.c}$ (Fig. 5, B and C). Within the medium expression group, nearly all

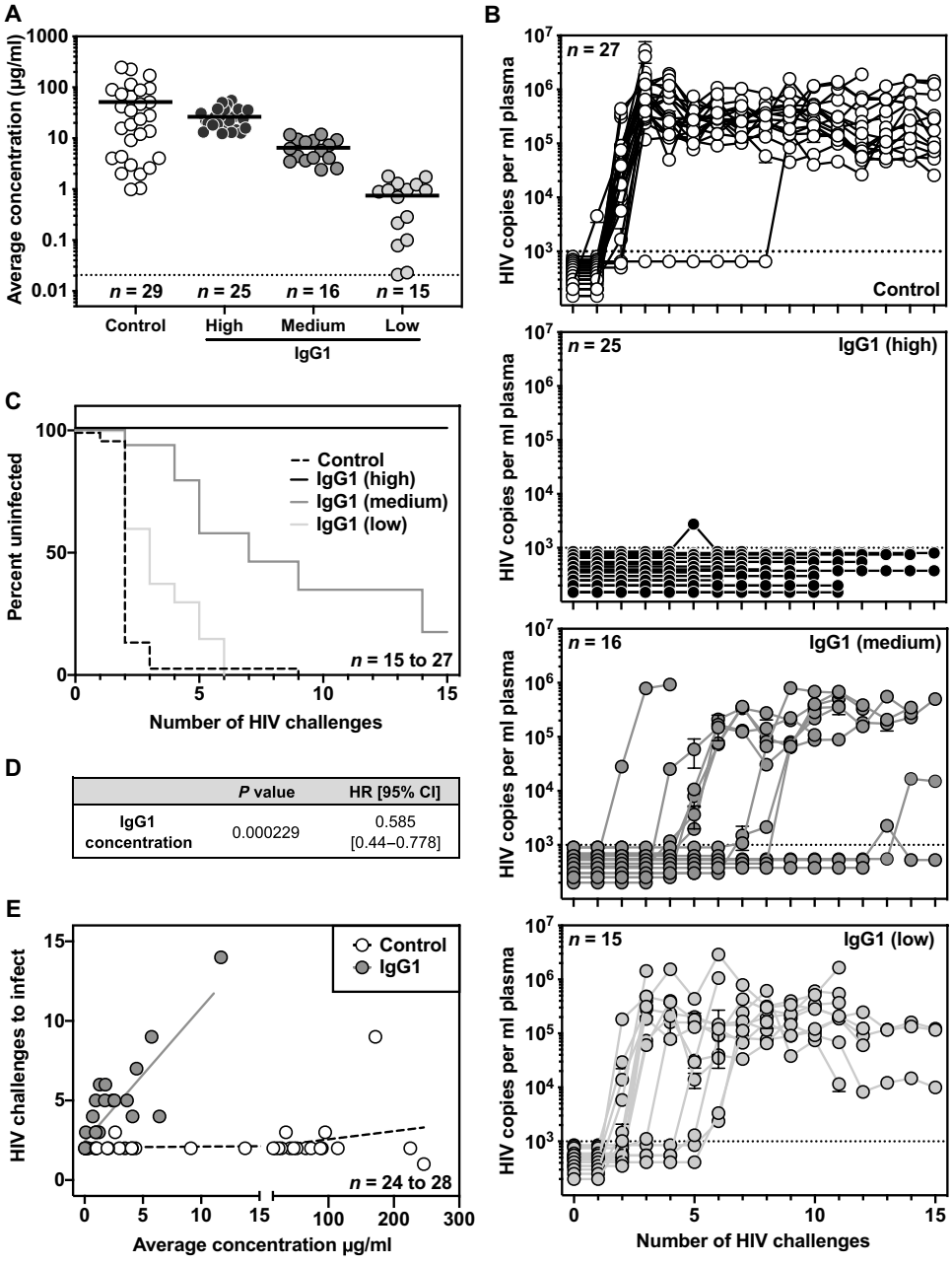

Fig. 5. Low concentrations of VRC07 IgG1 protect against repetitive HIV vaginal challenge in BLT humanized mice. (**A**) Average plasma antibody concentrations achieved in BLT mice from the start of vaginal challenge through HIV acquisition or death are shown. Mice given AAV-VRC07-IgG1 were grouped on the basis of the average plasma VRC07 concentration achieved over the course of challenge. High, greater than 12 μg/ml; medium, 2 to 10 μg/ml; low, less than 2 μg/ml. Malaria-specific negative control IgG1 antibody concentrations were determined using a separate ELISA protocol. The graphs represent combined data from three separate BLT experiments. Horizontal bars indicate the mean. The horizontal dotted line indicates the limit of detection, 0.02 μg/ml, for the assay. (**B**) Viral load in the peripheral blood of BLT mice was measured by qPCR. The dotted line indicates the limit of detection (1000 copies/ml) for the assay. (**C**) Kaplan-Meier survival curves are shown for mice expressing a malaria-specific control IgG1 antibody or varying concentrations of VRC07 IgG1. (**D**) Cox regression analysis was used to evaluate the effect of VRC07 IgG1 concentration on the rate of HIV acquisition across multiple BLT experiments. (**E**) The relationship between the average circulating antibody concentration (micrograms per milliliter) and the number of HIV challenges required for HIV infection to occur over the course of challenge in BLT humanized mice was plotted. Lines represent the result of a linear regression for mice expressing VRC07 IgG1 ($n = 24$ mice) or a malaria-specific negative control IgG1 ($n = 28$ mice).

mice expressing VRC07 of at least 6.5 μg/ml were fully protected, with a single exception that became infected after 14 repeated challenges. Even mice with circulating antibody concentrations as low as 3 to 5 μg/ml exhibited delays in HIV acquisition, becoming infected only after five or more repeated challenges. In contrast, mice expressing less than 1 μg/ml typically became infected after three repeated challenges, similar to mice expressing a negative control IgG1 antibody. However, three mice expressing VRC07 of between 0.95 and 1.78 μg/ml delayed HIV acquisition until five or six repeated challenges.

Overall, these findings are consistent with a dose-dependent effect of VRC07 IgG1 against $HIV_{REJO.c}$ challenge, with even relatively low plasma concentrations affording robust protection from vaginal transmission of this sensitive strain. A Cox regression analysis performed across this range of antibody concentrations found a statistically significant association ($P = 0.000229$) between the rate of HIV acquisition and VRC07 IgG1 concentration with a hazard ratio of 0.585, indicating that every 1 μg/ml increase in circulating antibody concentration resulted in a 1.71-fold decreased risk of HIV infection (Fig. 5D). In contrast, animals expressing a negative control IgG1 antibody exhibited no relationship between antibody concentration and the number of challenges required to become infected (Fig. 5E).

DISCUSSION

Through IgG subclass-switching and site-directed mutagenesis, we generated VRC07 IgG variants with differing capacities to elicit Fc-dependent functions. Despite their similarity in binding cell surface Env and neutralizing viral particles, these variants had substantially altered affinity for FcγRs. Consequently, VRC07 variants demonstrated markedly different ability to mediate ADCC and ADCP functions in vitro as measured in cell-based assays.

In an effort to deconvolute the contribution of individual IgG subclasses during prophylaxis, we assessed the ability of each subclass to mediate protection in vivo. Whereas all subclasses demonstrated the capacity for preventing HIV infection when present at high concentration during intravenous challenge, we found that VRC07 IgG2 exhibited markedly reduced protection against vaginal challenge in BLT humanized mice. Although some BLT mice expressing VRC07-IgG2 exhibited delays in HIV acquisition, substantially higher plasma antibody concentrations were necessary to achieve this outcome as compared with other subclasses. VRC07-IgG2 was the only subclass unable to mediate either ADCP or ADCC activity in vitro. Our findings support a model in which neutralization is sufficient to mediate protection at high circulating antibody concentrations, with Fc-dependent functions contributing to antibody efficacy near the minimum protective dose. This holds particular relevance for vaccine efforts where, if successful, the elicitation of bNAbs will likely occur at low titer.

In our studies, both IgG4 and IgG1-LALA conferred in vivo protection comparable to that of IgG1, suggesting that ADCC activity is insufficient to explain the differences observed in our model. Other studies in macaques have shown no appreciable differences in bNAb efficacy after NK cell depletion (*10*). Furthermore, a b12 variant with enhanced FcγR3a binding and ADCC activity failed to improve protection against mucosal $SHIV_{SF162P3}$ challenge in rhesus macaques (*33*). VRC07 IgG2 was the only subclass entirely lacking phagocytic activity in vitro. IgG2, IgG4, and LALA all exhibited a substantial reduction in affinity for FcγR2a compared to VRC07 IgG1. However, IgG2 was the only Fc variant also lacking FcγR1a binding. As a result, IgG4 and LALA maintained some ability to mediate phagocytosis of $HIV_{REJO.c}$ Env-expressing target cells. Furthermore, both IgG4 and LALA conferred protection against vaginal HIV challenge similar to more functional subclasses, suggesting that ADCP may be crucially important during antibody-mediated prevention of HIV transmission.

In support of this hypothesis, human clinical trials and NHP studies have also suggested ADCP as a potential mechanism of HIV prevention with other vaccine modalities (*34*). The HVTN 505 vaccine trial lacked overall efficacy but found that ADCP by monocytes correlated with decreased HIV risk (*35*). Similarly, IgG-driven monocyte-mediated phagocytosis correlated with reduced risk of SIV infection (*36*). Furthermore, an adjuvant enhancing antibody-dependent monocyte and neutrophil-mediated phagocytic responses augmented protection against stringent mucosal SHIV challenge in rhesus macaques (*37*).

Although we do not know the immune cell subset(s) responsible for driving ADCP activity in BLT humanized mice, we have demonstrated that human monocytes in this model express FcγRs and differentially bind to VRC07 Fc variants. A study of human biopsy samples found that FcγR-expressing macrophages were highly enriched in most tissues and that FcγR-expressing neutrophils mediated the most efficient phagocytosis (*38*). This study also found negligible FcγR-expressing NK cells in the female reproductive mucosa and other vulnerable tissues, suggesting that phagocytosis may be more likely to contribute to prevention (*38*). Additional studies will be necessary to dissect the precise effector mechanisms and immune cell populations contributing most to bNAb-mediated protection.

Our laboratory has previously shown that a variant of VRC07 IgG1 protected BLT mice from 21 repeated $HIV_{REJO.c}$ challenges when expressed at nearly 100 μg/ml in circulation (*17*). The present study demonstrates that wild-type VRC07 IgG1 concentrations eightfold lower than previously published still achieved complete protection from 15 consecutive $HIV_{REJO.c}$ challenges. VRC07-IgG1 of as little as 1 μg/ml in circulation substantially delayed HIV acquisition in BLT mice, suggesting that small amounts of functional bNAbs could have a meaningful impact on the transmission of neutralization-sensitive HIV strains. This is particularly relevant in light of progress made in the clinical translation of VIP to humans, given reports of durable expression of concentrations of VRC07 IgG1 at micrograms per milliliter in patients after vector administration in the VRC603 study (*39*).

Despite a median inhibitory concentration (IC_{50}) value of VRC07 against $HIV_{REJO.c}$ of 0.05 μg/ml in vitro, our in vivo challenge studies demonstrated that all mice expressing VRC07 of greater than 12 μg/ml were completely protected from vaginal $HIV_{REJO.c}$ challenge. This observation suggests that optimal efficacy in vivo requires a VRC07 IgG1 plasma concentration about 240 times higher than the in vitro IC_{50}. However, our study used a stringent challenge that led to infection of nearly all control mice after one to two challenges. In contrast, human heterosexual transmission is estimated to occur at a frequency between 1 in 100 and 1 in 1000 exposures (*40*, *41*). Therefore, our challenge regimen may reflect a high bar for antibody-mediated protection, possibly overestimating the concentration necessary for complete efficacy in humans.

Overall, our findings support the conclusion that IgG subclass contributes to bNAb-mediated HIV prevention through its role modulating antibody-dependent innate effector functions. This observation

is in agreement with mucosal challenge studies in rhesus macaques in which LALA exhibited reduced b12 antibody activity against vaginal $SHIV_{SF162P3}$ challenge (*8*). However, more recent work reported that Fc-dependent functions did not contribute to the protective efficacy of PGT121 in pigtail macaques, where PGT121-LALA completely protected animals from intravenous challenge with splenocytes from a $SHIV_{SF162P3}$-infected donor animal (*10*). Even at lower circulating antibody concentrations, PGT121 and PGT121-LALA demonstrated comparable protective efficacy against high-dose vaginal challenge of $SHIV_{SF162P3}$ (*9*). Given the results of our study, it will be essential that future experiments investigating the role of Fc function in bNAb efficacy compare Fc variant antibodies at a range of circulating antibody concentrations, encompassing the minimum protective dose for the specific model being used.

Our study has some limitations. The main focus of this study was to determine the role of IgG subclass during prevention of HIV transmission. For this purpose, we used several humanized mouse models that may not entirely recapitulate the immune environment of mucosal tissues in humans, possibly altering the efficiency of HIV transmission in the model and affecting the estimate of minimum protective dose for a given antibody. In particular, the relative scarcity of NK cells in the BLT model as compared to humans may underestimate the role of ADCC during antibody-mediated prevention. In addition, the functional potential of the innate cells within a BLT environment prone to developing GVHD has not been addressed, further contributing to a possible underestimation of their role in protection. Genetic variability between donors of tissues used to create the humanized mice in this study may have affected the influence of the innate immune system or bNAb prevention. In addition, vectored delivery and production from cells other than B cells may result in antibodies with different glycosylation patterns than those elicited naturally, which may influence their function. Last, the use of a challenge regimen resulting in productive HIV infection at a rate well above that seen in humans may underestimate the capacity for bNAbs to prevent infection, resulting in an overestimation of the minimum protective dose.

In conclusion, our findings suggest that IgG subclass is important for optimal prophylactic intervention against HIV, particularly at low bNAb concentrations. A maximally effective HIV antibody will likely be capable of broad, potent neutralization and substantial effector function activity to maximize its potential to prevent infection at lower concentrations. Future work defining the precise effector mechanisms involved in bNAb-mediated protection will be crucial to the design of optimally effective antibody-based interventions.

MATERIALS AND METHODS

Study design

The research aims of this study were to determine whether IgG subclass affects innate functionality of VRC07 and whether BLT humanized mice would reveal analogous differences in VRC07 protective efficacy. To this end, the impact of changes to VRC07 IgG subclass was assessed in vitro using Env-expressing cell lines to simulate recognition of infected target cells and in BLT humanized mice repetitively challenged intravaginally with low doses of transmitted founder HIV. BLT mouse group sizes were determined in consultation with statisticians to maximize statistical power of group comparisons with the minimum number of animals. To account for genetic variability between batches, in vivo experiments were performed in three groups of BLT mice and analyzed together. Mice were randomized to each treatment group, and studies were performed without blinding. Animals meeting predefined thresholds for health status were euthanized if showing signs of distress.

Human participants

The use of human tissues was approved by Partners Human Research Committee of Massachusetts General Hospital (MGH; protocol 2012P000409). All donor tissues were obtained under an MGH Institutional Review Board–approved protocol for discarded, deidentified tissues from participants who agreed to use of donations for research. Participants received no compensation.

Construction and purification of VRC07 Fc variant antibodies

Class-switched VRC07 constructs were generated from human isotype backbone plasmids obtained from Addgene. The different human heavy-chain constant regions were amplified from the Addgene plasmids by polymerase chain reaction (PCR) and inserted into the previously described AAV transfer vector (*16*) encoding the VRC07 heavy-chain variable region and VRC07 kappa light chain. Sequencing was performed to confirm constant region insertion. Subsequently, each class-switched VRC07 gene was cloned into a third-generation self-inactivating lentiviral vector. Lentivirus was produced by cotransfection of 293T cells with the given VRC07 IgG lentiviral vector and two helper plasmids (pHDM-VSV-G and pHDM-Hgpm2). After 48 hours, the culture supernatant containing lentivirus was collected, filtered, and used to transduce fresh 293T cells to generate cell lines stably expressing VRC07 IgG antibodies. These cell lines were incubated in FreeStyle 293 expression medium (Thermo Fisher Scientific) at 37°C for 10 to 15 days. VRC07 IgG antibodies were then purified from the culture supernatant using affinity chromatography with Pierce Protein A/G Agarose (Thermo Fisher Scientific) followed by size exclusion chromatography using a Superdex 200 column (GE Healthcare) on an AKTA Purifier Fast Protein Liquid Chromatography system (GE Healthcare). Quantification of purified protein was performed using a NanoDrop 2000 Spectrophotometer (Thermo Fisher Scientific) and an IgG-specific enzyme-linked immunosorbent assay (ELISA) with subclass-matched standards. To confirm the size of Fc variant antibodies, 1 μg of each purified protein was denatured under reducing conditions using β-mercaptoethanol and run on an SDS–polyacrylamide gel electrophoresis gel with the Precision Plus Protein standard (Bio-Rad).

HIV production and quantification

Viruses were produced by transient transfection of 293T cells with plasmid (2 μg/ml) encoding HIV_{NL4-3}, HIV_{JR-CSF}, or $HIV_{REJO.c}$ [National Institutes of Health (NIH) AIDS Reagent Program]. After 48 hours, culture supernatants were collected, filtered with a 0.45-μm filter, and titered using both an HIV-1 p24 antigen capture assay (Leidos Biomedical Research) and 50% tissue culture infective dose ($TCID_{50}$) assay on TZM-bl cells. $TCID_{50}$ was calculated using the Spearman-Karber formula (*42*).

In vitro neutralization assay

Neutralization assays were performed in quadruplicate by combining 200 $TCID_{50}$ of virus with threefold serial dilutions of a given antibody. Virus-antibody mixtures were incubated at 37°C for 1 hour.

After incubation, the mixtures were added to 96-well plates seeded with 10,000 TZM-bl cells per well 24 hours before the assay. Medium in each well was also supplemented with diethylaminoethyl dextran (75 μg/ml) to facilitate viral infection. After 48 hours at 37°C, cells were lysed using a previously described luciferase buffer (*43*), and luciferase expression was measured on a SpectraMax L microplate reader (Molecular Devices). Percent neutralization was calculated by subtracting the background luciferase signal of control wells (cells only) from the luciferase signal of experimental wells (cells with virus and antibody) and then dividing this value by the difference between virus control wells (cells with virus in the absence of antibody) and control wells with cells only.

Engineered CEM.NKr cells expressing cell surface HIV Env

CEM.NKr cells were obtained from the NIH AIDS Reagent Program and engineered to express $HIV_{JR\text{-}CSF}$ or $HIV_{REJO.c}$ Env using lentiviral transduction. Briefly, the gene for membrane-bound HIV gp150 was engineered for enhanced expression through human codon optimization and replacement of the endogenous Env leader sequence with the leader sequence of human CD5 antigen (*44*). The engineered $HIV_{JR\text{-}CSF}$ or $HIV_{REJO.c}$ gp150 gene was synthesized [Integrated DNA Technologies (IDT)] and cloned into a lentiviral vector (*45*). The transgene was expressed under control of the human elongation factor 1α promoter. An internal ribosome entry site located downstream of the envelope transgene and drove cap-independent translation of the fluorescent protein, ZsGreen. Lentivirus was produced through cotransfection of 293T cells with either the $HIV_{JR\text{-}CSF}$ or $HIV_{REJO.c}$ gp150 lentiviral vector and four helper plasmids (pHDM-VSV-G, pHDM-Hgpm2, pHDM-Tat1b, and pRC-CMV-Rev1b). After 48 hours, cell culture supernatants were collected, filtered through a 0.45-μm filter, and used to transduce CEM.NKr cells. After transduction, CEM.NKr cells were single-cell–sorted using a FACSAria II SORP Flow Cytometer (BD Biosciences) and screened on the basis of high Env and ZsGreen expression to generate a clonal target cell population.

In vitro effector function assays

Binding of VRC07 Fc variants to purified FcγR proteins was measured using a flow-based assay as previously described (*20*). $HIV_{JR\text{-}CSF}$ Env-expressing target cells were stained in triplicate with threefold serial dilutions of a given antibody for 30 min at room temperature followed by an FcγR detection reagent (0.65 μg/ml) for 1 hour at room temperature. The tetrameric detection reagents were generated immediately before use by combining biotinylated FcγR proteins (Ackerman Laboratory) with a 1:4 molar ratio of streptavidin-allophycocyanin (APC) (ProZyme) and mixing by inversion for 10 min. Free biotin was then added to a final concentration of 5 μM to completely block free streptavidin binding sites. The stained samples were analyzed on a Stratedigm S1300Exi flow cytometer. To determine the EC_{50} of each antibody, the mean fluorescence intensity (MFI) of APC and antibody concentrations were log-transformed and fit with a nonlinear regression using variable slope function in GraphPad Prism.

To measure ADCP, a bead-based assay was used as previously described (*20*, *21*). Briefly, purified $HIV_{JR\text{-}CSF}$ or $HIV_{REJO.c}$ gp120 protein was biotinylated using EZ-Link Sulfo-NHS-LC-Biotin (Thermo Fisher Scientific), and excess biotin was removed using a Zeba spin desalting column (Thermo Fisher Scientific). Biotinylated antigen was then conjugated to fluorescent neutravidin-labeled microspheres. The gp120-conjugated beads were incubated in triplicate with fivefold serial dilutions of a given antibody for 2 hours at 37°C in 96-well plates. After incubation, 25,000 THP-1 cells (American Type Culture Collection) were added to each well in a final volume of 200 μl, and plates were incubated at 37°C overnight. Cells were then analyzed on a Stratedigm S1300Exi flow cytometer, and a phagocytosis score was calculated by multiplying the percent of bead-positive THP-1 cells by the MFI of the bead-positive cell population.

In addition to the bead-based ADCP assay, a cell-based assay was performed using $ZsGreen^+$ $HIV_{JR\text{-}CSF}$ or $HIV_{REJO.c}$ Env-expressing CEM.NKr cell lines. Briefly, these target cells were mixed with parental CEM.NKr cells at a 1:1 ratio followed by threefold serial dilutions of a given antibody in triplicate. After 15 min at room temperature, THP-1 cells stained with CellTrace Violet were added at a 1:1 effector:target ratio, and the cocultures were incubated at 37°C overnight. The following day, cells were washed with 1× phosphate-buffered saline (PBS) and then fixed with 4% paraformaldehyde (PFA) for 20 min. Cells were analyzed on a Stratedigm S1300Exi flow cytometer, and phagocytosis score was calculated by multiplying the percent of $ZsGreen^+$ THP-1 cells by the MFI of the $ZsGreen^+$ cell population.

To measure ADCC, $HIV_{JR\text{-}CSF}$ or $HIV_{REJO.c}$ Env-expressing CEM.NKr cells were combined with parental CEM.NKr cells at a 1:1 ratio. The mixed target population was then incubated with fivefold serial dilutions of a given antibody in triplicate for 30 min at room temperature. After incubation, NK cells isolated from buffy coats using an EasySep human NK cell enrichment kit (STEMCELL Technologies) were added to the mixed target population at a 1:1 effector:target ratio. Before addition, NK cells were stained with CellTrace Violet for 20 min at room temperature. Phycoerythrin (PE)/cyanine7 (Cy7)–conjugated anti-human CD107a antibody (BioLegend) was added to each effector-target cell mixture at a final concentration of 2 to 3 μg/ml, and plates were incubated at 37°C for 6 hours. After incubation, cells were stained with LIVE/DEAD Fixable Far Red dye at a 1:1000 dilution from stock (Thermo Fisher Scientific), fixed with BD Cytofix fixation buffer (BD Biosciences), and analyzed on a Stratedigm S1300Exi flow cytometer. Degranulation of NK cells was measured as the percent of live, $CD107a^+$, $CellTrace\ Violet^+$ cells. Specific cell killing was measured by reduction in the percentage of the live, $ZsGreen^+$ CEM.NKr cells in the target population.

Animals

Immunodeficient NOD/SCID IL2Rgamma^{null} (NSG) mice were obtained from The Jackson Laboratory. To generate huPBMC-engrafted NSG mice, frozen huPBMCs (AllCells) were thawed and expanded in RPMI 1640 medium (Sigma-Aldrich) supplemented with 10% fetal bovine serum (FBS; VWR International), 1% L-glutamine (Thermo Fisher Scientific), 10 mM Hepes (Corning Inc.), 1× nonessential amino acids (Corning Inc.), 1× sodium pyruvate (Corning Inc.), 50 μM β-mercaptoethanol (Agilent Technologies), and 1% penicillin-streptomycin (Corning Inc.) and stimulated for T cell expansion with phytohemagglutinin (5 μg/ml; Sigma-Aldrich) and human interleukin-2 (10 ng/ml). After 10 days of in vitro expansion, 4 million cells were administered to NSG mice by intraperitoneal injection in a 300-μl volume. Mice were rested 2 weeks after cell administration to allow for engraftment.

BLT humanized mice were generated by the Human Immune System Mouse Program at the Ragon Institute of MGH, MIT, and

Harvard. Briefly, 6- to 8-week-old female NSG mice were transplanted with human liver and thymus tissue under the kidney capsule and injected intravenously with 100,000 $CD34^+$ cells isolated from liver tissue by AutoMACS (Miltenyi Biotec). Mice were rested 10 weeks after surgery to allow for recovery and engraftment. All experiments were done with approval from the Institutional Animal Care and Use Committee of the MGH and conducted in accordance with the regulations of the American Association for the Accreditation of Laboratory Animal Care.

Flow cytometry of mouse samples for FcγR expression profiling

Ten weeks after surgery, blood samples were taken from BLT mice by retro-orbital bleeding and centrifuged at 1150*g* for 5 min at room temperature to separate plasma from the cell pellets. Plasma was removed and frozen at −80°C for subsequent analysis. The cell pellets were resuspended in 1.1 ml of 1× red blood cell (RBC) lysis buffer (BioLegend) and incubated on ice for 10 min. After RBC lysis, each sample was pelleted at 1150*g* in a centrifuge for 5 min at room temperature and then stained with 50 μl of an antibody cocktail containing 1:50 diluted anti-human CD45–Alexa Fluor (AF) 700 (BioLegend, clone HI30), 1:100 diluted anti-human CD3- fluorescein isothiocyanate (FITC) (BioLegend, clone UCHT1), 1:25 diluted anti-human CD19-PE/Cy7 (BioLegend, clone SJ25C1), 1:25 diluted anti-human CD56–Brilliant Violet (BV) 570 (BioLegend, clone HCD56), 1:25 diluted anti-human CD14-PE (BioLegend, clone HCD14), 1:25 diluted anti-human CD11c-BV421 (BioLegend, clone Bu15), 1:50 diluted anti-human HLA-DR-BV510 (BioLegend, clone L243), 1:50 diluted anti-human CD16-APC/Cy7 (BioLegend, clone B73.1), 1:50 diluted anti-human CD32-APC (BioLegend, clone FUN-2), and 1:50 diluted anti-human CD64-PE/DAZZLE594 (BioLegend, clone 10.1) in PBS supplemented with 2% FBS (PBS^+) for 30 min on ice. Samples were then analyzed on a Stratedigm S1300Exi flow cytometer. T cells were defined as a $CD45^+$, $CD3^+$ population. B cells were defined as a $CD45^+$, $CD19^+$ population. NK cells were defined as a $CD45^+$, $CD3^-$, $CD19^-$, HLA-DR^-, $CD56^+$ population. Myeloid cells were defined as a $CD45^+$, $CD3^-$, $CD19^-$, $CD11c^+$, HLA-DR^+ population. The frequency of FcγR expression (CD64, CD32, and CD16) was then assessed for each cell population.

Flow cytometry of mouse samples for VRC07 subclass staining of myeloid populations

Spleens were harvested from BLT mice at 25 weeks or 34 weeks after surgery and washed twice with complete RPMI 1640 at 500*g*. HuPBMCs were isolated from whole blood by histopaque density gradient centrifugation (Sigma-Aldrich). Cells were stained with VRC07-AF647–conjugated isotypes (1.75 μg/ml) VRC07-IgG1, VRC07-IgG2, VRC07-IgG3, VRC07-IgG4, and VRC07-IgG1-LALA at 4°C for 30 min in PBS. Cells were washed with PBS supplemented with 2% FBS (PBS^+) and then stained with 50 μl of an antibody cocktail containing 1:50 diluted anti-human CD45-AF700 (BioLegend, clone HI30), 1:50 diluted anti-human CD3-BV605 (BioLegend, clone UCHT1), 1:50 diluted anti-human CD20-BV650 (BioLegend, clone 2H7), 1:50 diluted anti-human HLA-DR-BV570 (BioLegend, clone L243), 1:50 diluted anti-human CD15-PE/Cy5 (BioLegend, clone W6D3), 1:50 diluted anti-human CD13-PerCP/Cy5.5 (BioLegend, clone WM15), 1:50 diluted anti-human CD16-BV785 (BioLegend, clone 3G8), 1:50 diluted anti-human CD14-PE/Cy7 (BioLegend, clone M5E2), 1:50 diluted anti-human CD11b-BV421 (BioLegend, clone LM2), 1:50 diluted anti-human CD11c-FITC (BD Biosciences, clone B-ly6), 1:50 diluted anti-human CD56-PE (BioLegend, clone QA17A16), and 1:100 diluted LIVE/DEAD near IR in PBS^+ for 30 min at 4°C. Samples were then washed and fixed in 4% PFA and analyzed on a Stratedigm S1300Exi flow cytometer. T cells were defined as a $CD45^+$, $CD3^+$ population. B cells were defined as a $CD45^+$, $CD20^+$ population. NK cells were defined as a $CD45^+$, $CD3^-$, $CD14^-$, $CD11c^-$, $CD56^+$ population. Classical monocytes were defined as a $CD45^+$, CD3-, $CD56^-$, $CD15^-$, $CD16^-$, $CD14^+$ population. Macrophages were defined as a $CD45^+$, $CD3^-$, CD56-, $CD14^+$, $CD16^+$, $CD64^+$, $CD11b^+$ population. Neutrophils were defined as a $CD45^+$, $CD3^-$, CD56-, $CD15^+$, $CD13^+$ population. DCs were defined as a $CD45^+$, $CD3^-$, $CD56^-$, $CD14^-$, $CD16^-$, HLA-DR^+, $CD11c^+$ population. VRC07 engagement with specific cell types was shown as histograms, and the MFI of AF647 was calculated for each isotype staining.

AAV virus production, quantification, and administration

AAV2/8 encoding a given antibody was produced by transient transfection of 293T cells and purification from the culture supernatant by polyethylene glycol precipitation and cesium chloride ultracentrifugation as previously described (*16*). AAV titers were then determined by quantitative PCR (qPCR). Briefly, AAV aliquots were serially diluted and incubated with 1.2 U of Turbo deoxyribonuclease (DNase) (Invitrogen) for 30 min at 37°C. DNase-treated virus (5 μl) was used in a 15-μl qPCR reaction with PerfeCTa SYBR Green SuperMix, ROX (Quanta Biosciences), and primers were designed against the CMV enhancer (5′-AACGCCAATAGGGACTTTCC and 3′-GGGCGTACTTGGCATATGAT). Samples were run in duplicate on a QuantStudio 12K Flex Real-Time PCR system (Applied Biosystems) with the following cycling conditions: 50°C for 2 min, 95°C for 10 min, followed by 50 cycles of 95°C for 15 s and 60°C for 60 s. Virus titer was determined by comparison with a standard curve generated using AAV transfer vector plasmid DNA. Intramuscular injections of titered AAV were performed as previously described (*16*). Briefly, aliquots of virus were thawed on ice and diluted to the desired dose in a 40-μl volume. A single injection of 40 μl was administered into the gastrocnemius muscle of NSG mice or BLT humanized mice using a 28-gauge insulin syringe.

HIV challenge of humanized mice

HuPBMC-NSG mice were challenged with 280 $TCID_{50}$ HIV_{NL4-3} in a 50-μl volume 2 weeks after humanization with PBMCs. Intravenous challenge was administered through retro-orbital injection of the venous sinus using a 28-gauge insulin syringe. BLT mice were challenged with 30 ng of p24 $HIV_{REJO.c}$ in a 20-μl volume. Vaginal challenge was performed nonabrasively by placing isoflurane-anesthetized mice in a supine position and elevating the posterior of the animal before shallow insertion of the pipette loaded with virus into the vaginal vault. After viral administration, mice were maintained in a supine position for 5 min to prevent loss of the virus. This vaginal challenge protocol was repeated weekly until the conclusion of the experiment. For all mouse experiments, mice were bled weekly to determine $CD4^+$ T cell counts, plasma antibody concentrations, and plasma viral loads.

Flow cytometry of blood samples

Blood samples were taken from mice by retro-orbital bleeding and centrifuged at 1150*g* for 5 min at room temperature to separate plasma from the cell pellets. Plasma was removed and frozen at

−80°C for subsequent analysis. The cell pellets were resuspended in 1.1 ml of 1× RBC lysis buffer (BioLegend) and incubated on ice for 10 min. After RBC lysis, each sample was pelleted at 1150*g* in a centrifuge for 5 min at room temperature and then stained with 50 μl of an antibody cocktail containing 1:100 diluted anti-human CD3-FITC (BioLegend, clone UCHT1), 1:100 diluted anti-human CD4-PE (BioLegend, clone RPA-T4), and 1:100 diluted anti-human CD8-APC (BioLegend, clone RPA-T8) in PBS^+ for 30 min on ice. Samples were then analyzed on a Stratedigm S1000 flow cytometer. Samples were first gated by CD3 expression before determining the ratio of CD4 to CD8 within this subset. Samples containing fewer than 20 $CD3^+$ events were excluded from the analysis.

Antibody quantification by ELISA

For detection of gp120-binding IgG in mouse serum samples, ELISA plates were coated with 0.2 μg per well of purified $HIV_{JR\text{-}CSF}$ gp120 protein for 1 hour at room temperature. Plates were then blocked with 1% bovine serum albumin (BSA; KPL) in tris-buffered saline (TBS) for at least 30 min at room temperature or overnight at 4°C. Mouse serum samples were diluted in TBS plus Tween 20 containing 1% BSA (KPL) and incubated on the plate for 1 hour at room temperature, followed by a 30-min incubation with horseradish peroxidase–conjugated goat anti-human IgG Fc antibody at a 1:2500 dilution (Bethyl, A80-104A). Detection was completed using the TMB Microwell Peroxidase Substrate System (KPL) and a VersaMax microplate reader (Molecular Devices). Samples were compared to a standard curve generated using purified VRC07 antibodies of the same IgG subclass.

Viral load quantification by RT-qPCR

Viral RNA was extracted from mouse serum using the QIAGEN QIAamp Viral RNA Mini Kit. Each RNA sample was treated with 2 U of Turbo DNase (Invitrogen) for 30 min at 37°C, followed by 15 min at 75°C for heat inactivation. To quantify viral RNA, 10 μl of the DNase-treated sample was used in a 20-μl reverse transcription (RT)–qPCR reaction with qScript XLT one-step RT-qPCR ToughMix low-ROX (Quanta Biosciences), a TaqMan probe (5′-/56-FAM/CCCACCAAC/ZEN/AGGCGGCCTTAACTG/3IABkFQ/-3′) (IDT), and primers were designed to target the Pol gene of $HIV_{REJO.c}$ (5′-CAATGGCCCCAATTTCATCA and 3′- GAATGCCGAATTCCTGCTTGA) or $HIV_{NL4\text{-}3}$ (5′-CAATGGCAGCAATTTCACCA and 3′-GAATGCCAAATTCCTGCTTGA). Samples were run in triplicate on a QuantStudio 12K Flex Real-Time PCR system (Applied Biosystems) with the following cycle conditions: 50°C for 10 min, 95°C for 3 min followed by 55 cycles of 95°C for 3 s and 60°C for 30 s. Virus titer was determined by comparison with a standard curve generated using RNA extracted from a serially diluted mixture of commercially titered viral stock and pure mouse serum. For all viral strains, the limit of detection was 1000 HIV genome copies/ml.

Statistical analysis

Data were plotted using Prism 9 (GraphPad Software), and statistical analysis of in vitro studies was performed with included tools. The survival data were fit to a cox proportional hazards regression model using the coxph function from the survival package v3.2-7 (https://CRAN.Rproject.org/package=survival) in R v4.0.2 (R Core Team 2020). An infection event was defined as two consecutive positive viral loads, and the week of the first positive sample was defined as the time of HIV acquisition. All mice that survived at least 7 weeks after AAV administration were included in the analysis. All data from experiments contained in this study are provided as data file S1.

SUPPLEMENTARY MATERIALS

www.science.org/doi/10.1126/scitranslmed.abn9662
Figs. S1 to S10
Tables S1 and S2
MDAR Reproducibility Checklist
Data file S1

View/request a protocol for this paper from *Bio-protocol*.

REFERENCES AND NOTES

1. C. A. Janeway, P. Travers, M. Walport, M. J. Shlomchik, C. A. J. Jr, P. Travers, M. Walport, M. J. Shlomchik, *Immunobiology* (Garland Science, ed. 5, 2001).
2. G. Vidarsson, G. Dekkers, T. Rispens, IgG Subclasses and Allotypes: From structure to effector functions. *Front. Immunol.* **5**, 520 (2014).
3. L. Corey, P. B. Gilbert, M. Juraska, D. C. Montefiori, L. Morris, S. T. Karuna, S. Edupuganti, N. M. Mgodi, A. C. deCamp, E. Rudnicki, Y. Huang, P. Gonzales, R. Cabello, C. Orrell, J. R. Lama, F. Laher, E. M. Lazarus, J. Sanchez, I. Frank, J. Hinojosa, M. E. Sobieszczyk, K. E. Marshall, P. G. Mukwekwerere, J. Makhema, L. R. Baden, J. I. Mullins, C. Williamson, J. Hural, M. J. McElrath, C. Bentley, S. Takuva, M. M. Gomez Lorenzo, D. N. Burns, N. Espy, A. K. Randhawa, N. Kochar, E. Piwowar-Manning, D. J. Donnell, N. Sista, P. Andrew, J. G. Kublin, G. Gray, J. E. Ledgerwood, J. R. Mascola, M. S. Cohen, Two randomized trials of neutralizing antibodies to prevent HIV-1 acquisition. *N. Engl. J. Med.* **384**, 1003–1014 (2021).
4. D. Sok, D. R. Burton, Recent progress in broadly neutralizing antibodies to HIV. *Nat. Immunol.* **19**, 1179–1188 (2018).
5. M. L. Visciano, M. Tagliamonte, M. L. Tornesello, F. M. Buonaguro, L. Buonaguro, Effects of adjuvants on IgG subclasses elicited by virus-like Particles. *J. Transl. Med.* **10**, 4 10.1186/1479-5876-10-4 (2012).
6. K. Banerjee, P. J. Klasse, R. W. Sanders, F. Pereyra, E. Michael, M. Lu, B. D. Walker, J. P. Moore, IgG subclass profiles in infected HIV type 1 controllers and chronic progressors and in uninfected recipients of Env vaccines. *AIDS Res. Hum. Retroviruses* **26**, 445–458 (2010).
7. S. Bournazos, F. Klein, J. Pietzsch, M. S. Seaman, M. C. Nussenzweig, J. V. Ravetch, Broadly neutralizing anti-HIV-1 antibodies require Fc effector functions for in vivo activity. *Cell* **158**, 1243–1253 (2014).
8. A. J. Hessell, L. Hangartner, M. Hunter, C. E. G. Havenith, F. J. Beurskens, J. M. Bakker, C. M. S. Lanigan, G. Landucci, D. N. Forthal, P. W. H. I. Parren, P. A. Marx, D. R. Burton, Fc receptor but not complement binding is important in antibody protection against HIV. *Nature* **449**, 101–104 (2007).
9. L. Hangartner, D. Beauparlant, E. Rakasz, R. Nedellec, N. Hozé, K. McKenney, M. A. Martins, G. E. Seabright, J. D. Allen, A. M. Weiler, T. C. Friedrich, R. R. Regoes, M. Crispin, D. R. Burton, Effector function does not contribute to protection from virus challenge by a highly potent HIV broadly neutralizing antibody in nonhuman primates. *Sci. Transl. Med.* **13**, eabe3349 (2021).
10. M. S. Parsons, W. S. Lee, A. B. Kristensen, T. Amarasena, G. Khoury, A. K. Wheatley, A. Reynaldi, B. D. Wines, P. M. Hogarth, M. P. Davenport, S. J. Kent, Fc-dependent functions are redundant to efficacy of anti-HIV antibody PGT121 in macaques. *J. Clin. Invest.* **129**, 182–191 (2019).
11. G. Alter, W.-H. Yu, A. Chandrashekar, E. N. Borducchi, K. Ghneim, A. Sharma, R. Nedellec, K. R. McKenney, C. Linde, T. Broge, T. J. Suscovich, T. Linnekin, P. Abbink, N. B. Mercado, J. P. Nkolola, K. McMahan, E. A. Bondzie, V. Hamza, L. Peter, N. Kordana, S. Mahrokhian, M. S. Seaman, W. Li, M. G. Lewis, D. A. Lauffenburger, L. Hangartner, R.-P. Sekaly, D. H. Barouch, Passive transfer of vaccine-elicited antibodies protects against SIV in Rhesus Macaques. *Cell* **183**, 185–196.e14 (2020).
12. A. R. Crowley, M. E. Ackerman, Mind the gap: How interspecies variability in IgG and its receptors may complicate comparisons of human and non-human primate effector function. *Front. Immunol.* **10**, 697 (2019).
13. B. Julg, L. J. Tartaglia, B. F. Keele, K. Wagh, A. Pegu, D. Sok, P. Abbink, S. D. Schmidt, K. Wang, X. Chen, M. G. Joyce, I. S. Georgiev, M. Choe, P. D. Kwong, N. A. Doria-Rose, K. Le, M. K. Louder, R. T. Bailer, P. L. Moore, B. Korber, M. S. Seaman, S. S. Abdool Karim, L. Morris, R. A. Koup, J. R. Mascola, D. R. Burton, D. H. Barouch, Broadly neutralizing antibodies targeting the HIV-1 envelope V2 apex confer protection against a clade C SHIV challenge. *Sci. Transl. Med.* **9**, eaal1321 (2017).
14. B. Moldt, E. G. Rakasz, N. Schultz, P.-Y. Chan-Hui, K. Swiderek, K. L. Weisgrau, S. M. Piaskowski, Z. Bergman, D. I. Watkins, P. Poignard, D. R. Burton, Highly potent

HIV-specific antibody neutralization in vitro translates into effective protection against mucosal SHIV challenge in vivo. *Proc. Natl. Acad. Sci. U.S.A.* **109**, 18921–18925 (2012).
15. A. Pegu, B. Borate, Y. Huang, M. G. Pauthner, A. J. Hessell, B. Julg, N. A. Doria-Rose, S. D. Schmidt, L. N. Carpp, M. D. Cully, X. Chen, G. M. Shaw, D. H. Barouch, N. L. Haigwood, L. Corey, D. R. Burton, M. Roederer, P. B. Gilbert, J. R. Mascola, Y. Huang, A meta-analysis of passive immunization studies shows that serum-neutralizing antibody titer associates with protection against SHIV challenge. *Cell Host Microbe* **26**, 336–346.e3 (2019).
16. A. B. Balazs, J. Chen, C. M. Hong, D. S. Rao, L. Yang, D. Baltimore, Antibody-based protection against HIV infection by vectored immunoprophylaxis. *Nature* **481**, 81–84 (2011).
17. A. B. Balazs, Y. Ouyang, C. M. Hong, J. Chen, S. M. Nguyen, D. S. Rao, D. S. An, D. Baltimore, Vectored immunoprophylaxis protects humanized mice from mucosal HIV transmission. *Nat. Med.* **20**, 296–300 (2014).
18. K. O. Saunders, L. Wang, M. G. Joyce, Z.-Y. Yang, A. B. Balazs, C. Cheng, S.-Y. Ko, W.-P. Kong, R. S. Rudicell, I. S. Georgiev, L. Duan, K. E. Foulds, M. Donaldson, L. Xu, S. D. Schmidt, J.-P. Todd, D. Baltimore, M. Roederer, A. T. Haase, P. D. Kwong, S. S. Rao, J. R. Mascola, G. J. Nabel, Broadly neutralizing human immunodeficiency virus type 1 antibody gene transfer protects nonhuman primates from mucosal simian-human immunodeficiency virus infection. *J. Virol.* **89**, 8334–8345 (2015).
19. H. C. Welles, M. F. Jennewein, R. D. Mason, S. Narpala, L. Wang, C. Cheng, Y. Zhang, J.-P. Todd, J. D. Lifson, A. B. Balazs, G. Alter, A. B. McDermott, J. R. Mascola, M. Roederer, Vectored delivery of anti-SIV envelope targeting mAb via AAV8 protects rhesus macaques from repeated limiting dose intrarectal swarm SIVsmE660 challenge. *PLOS Pathog.* **14**, e1007395 (2018).
20. E. P. Brown, K. G. Dowell, A. W. Boesch, E. Normandin, A. E. Mahan, T. Chu, D. H. Barouch, C. Bailey-Kellogg, G. Alter, M. E. Ackerman, Multiplexed Fc array for evaluation of antigen-specific antibody effector profiles. *J. Immunol. Methods* **443**, 33–44 (2017).
21. M. E. Ackerman, B. Moldt, R. T. Wyatt, A.-S. Dugast, E. McAndrew, S. Tsoukas, S. Jost, C. T. Berger, G. Sciaranghella, Q. Liu, D. J. Irvine, D. R. Burton, G. Alter, A robust, high-throughput assay to determine the phagocytic activity of clinical antibody samples. *J. Immunol. Methods* **366**, 8–19 (2011).
22. T. H. Chu, A. R. Crowley, I. Backes, C. Chang, M. Tay, T. Broge, M. Tuyishime, G. Ferrari, M. S. Seaman, S. I. Richardson, G. D. Tomaras, G. Alter, D. Leib, M. E. Ackerman, Hinge length contributes to the phagocytic activity of HIV-specific IgG1 and IgG3 antibodies. *PLOS Pathog.* **16**, e1008083 (2020).
23. S. I. Richardson, B. E. Lambson, A. R. Crowley, A. Bashirova, C. Scheepers, N. Garrett, S. Abdool Karim, N. N. Mkhize, M. Carrington, M. E. Ackerman, P. L. Moore, L. Morris, IgG3 enhances neutralization potency and Fc effector function of an HIV V2-specific broadly neutralizing antibody. *PLOS Pathog.* **15**, e1008064 (2019).
24. K. C. Kim, B.-S. Choi, K.-C. Kim, K. H. Park, H. J. Lee, Y. K. Cho, S. I. Kim, S. S. Kim, Y.-K. Oh, Y. B. Kim, A simple mouse model for the study of human immunodeficiency virus. *AIDS Res. Hum. Retroviruses* **32**, 194–202 (2016).
25. K. S. M. Yong, Z. Her, Q. Chen, Humanized mice as unique tools for human-specific studies. *Arch. Immunol. Ther. Exp. (Warsz.)* **66**, 245–266 (2018).
26. C. Ochsenbauer, T. G. Edmonds, H. Ding, B. F. Keele, J. Decker, M. G. Salazar, J. F. Salazar-Gonzalez, R. Shattock, B. F. Haynes, G. M. Shaw, B. H. Hahn, J. C. Kappes, Generation of transmitted/founder HIV-1 infectious molecular clones and characterization of their replication capacity in CD4 T lymphocytes and monocyte-derived macrophages. *J. Virol.* **86**, 2715–2728 (2012).
27. M. Hezareh, A. J. Hessell, R. C. Jensen, J. G. van de Winkel, P. W. Parren, Effector function activities of a panel of mutants of a broadly neutralizing antibody against human immunodeficiency virus type 1. *J. Virol.* **75**, 12161–12168 (2001).
28. P. W. Denton, J. D. Estes, Z. Sun, F. A. Othieno, B. L. Wei, A. K. Wege, D. A. Powell, D. Payne, A. T. Haase, J. V. Garcia, Antiretroviral pre-exposure prophylaxis prevents vaginal transmission of HIV-1 in humanized BLT mice. *PLOS Med.* **5**, e16 (2008).
29. C. A. Stoddart, E. Maidji, S. A. Galkina, G. Kosikova, J. M. Rivera, M. E. Moreno, B. Sloan, P. Joshi, B. R. Long, Superior human leukocyte reconstitution and susceptibility to vaginal HIV transmission in humanized NOD-scid IL-2Rγ(−/−) (NSG) BLT mice. *Virology* **417**, 154–160 (2011).
30. Z. Sun, P. W. Denton, J. D. Estes, F. A. Othieno, B. L. Wei, A. K. Wege, M. W. Melkus, A. Padgett-Thomas, M. Zupancic, A. T. Haase, J. V. Garcia, Intrarectal transmission, systemic infection, and $CD4^+$ T cell depletion in humanized mice infected with HIV-1. *J. Exp. Med.* **204**, 705–714 (2007).
31. J. S. Yi, M. Rosa-Bray, J. Staats, P. Zakroysky, C. Chan, M. A. Russo, C. Dumbauld, S. White, T. Gierman, K. J. Weinhold, J. T. Guptill, Establishment of normative ranges of the healthy human immune system with comprehensive polychromatic flow cytometry profiling. *PLOS ONE* **14**, e0225512 (2019).
32. C. Deal, A. B. Balazs, D. A. Espinosa, F. Zavala, D. Baltimore, G. Ketner, Vectored antibody gene delivery protects against Plasmodium falciparum sporozoite challenge in mice. *Proc. Natl. Acad. Sci. U.S.A.* **111**, 12528–12532 (2014).
33. B. Moldt, M. Shibata-Koyama, E. G. Rakasz, N. Schultz, Y. Kanda, D. C. Dunlop, S. L. Finstad, C. Jin, G. Landucci, M. D. Alpert, A.-S. Dugast, P. W. H. I. Parren, F. Nimmerjahn, D. T. Evans, G. Alter, D. N. Forthal, J. E. Schmitz, S. Iida, P. Poignard, D. I. Watkins, A. J. Hessell, D. R. Burton, A nonfucosylated variant of the anti-HIV-1 monoclonal antibody b12 has enhanced FcγRIIIa-mediated antiviral activity in vitro but does not improve protection against mucosal SHIV challenge in macaques. *J. Virol.* **86**, 6189–6196 (2012).
34. S. Shangguan, P. K. Ehrenberg, A. Geretz, L. Yum, G. Kundu, K. May, S. Fourati, K. Nganou-Makamdop, L. D. Williams, S. Sawant, E. Lewitus, P. Pitisuttithum, S. Nitayaphan, S. Chariyalertsak, S. Rerks-Ngarm, M. Rolland, D. C. Douek, P. Gilbert, G. D. Tomaras, N. L. Michael, S. Vasan, R. Thomas, Monocyte-derived transcriptome signature indicates antibody-dependent cellular phagocytosis as a potential mechanism of vaccine-induced protection against HIV-1. *eLife* **10**, e69577 (2021).
35. S. D. Neidich, Y. Fong, S. S. Li, D. E. Geraghty, B. D. Williamson, W. C. Young, D. Goodman, K. E. Seaton, X. Shen, S. Sawant, L. Zhang, A. C. deCamp, B. S. Blette, M. Shao, N. L. Yates, F. Feely, C.-W. Pyo, G. Ferrari; HVTN 505 Team, I. Frank, S. T. Karuna, E. M. Swann, J. R. Mascola, B. S. Graham, S. M. Hammer, M. E. Sobieszczyk, L. Corey, H. E. Janes, M. J. McElrath, R. Gottardo, P. B. Gilbert, G. D. Tomaras, Antibody Fc effector functions and IgG3 associate with decreased HIV-1 risk. *J. Clin. Invest.* **129**, 4838–4849 (2019).
36. M. E. Ackerman, J. Das, S. Pittala, T. Broge, C. Linde, T. J. Suscovich, E. P. Brown, T. Bradley, H. Natarajan, S. Lin, J. K. Sassic, S. O'Keefe, N. Mehta, D. Goodman, M. Sips, J. A. Weiner, G. D. Tomaras, B. F. Haynes, D. A. Lauffenburger, C. Bailey-Kellogg, M. Roederer, G. Alter, Route of immunization defines multiple mechanisms of vaccine-mediated protection against SIV. *Nat. Med.* **24**, 1590–1598 (2018).
37. K. Om, D. Paquin-Proulx, M. Montero, K. Peachman, X. Shen, L. Wieczorek, Z. Beck, J. A. Weiner, D. Kim, Y. Li, T. Mdluli, Z. Shubin, C. Bryant, V. Sharma, A. Tokarev, P. Dawson, Y. White, O. Appelbe, N. R. Klatt, S. Tovanabutra, J. D. Estes, G. R. Matyas, G. Ferrari, C. R. Alving, G. D. Tomaras, M. E. Ackerman, N. L. Michael, M. L. Robb, V. Polonis, M. Rolland, M. A. Eller, M. Rao, D. L. Bolton, Adjuvanted HIV-1 vaccine promotes antibody-dependent phagocytic responses and protects against heterologous SHIV challenge. *PLOS Pathog.* **16**, e1008764 (2020).
38. M. Sips, M. Krykbaeva, T. J. Diefenbach, M. Ghebremichael, B. A. Bowman, A.-S. Dugast, A. W. Boesch, H. Streeck, D. S. Kwon, M. E. Ackerman, T. J. Suscovich, P. Brouckaert, T. W. Schacker, G. Alter, Fc receptor-mediated phagocytosis in tissues as a potent mechanism for preventive and therapeutic HIV vaccine strategies. *Mucosal Immunol.* **9**, 1584–1595 (2016).
39. J. P. Casazza, E. M. Cale, S. Narpala, G. V. Yamshchikov, E. E. Coates, C. S. Hendel, L. Novik, L. A. Holman, A. T. Widge, P. Apte, I. Gordon, M. R. Gaudinski, M. Conan-Cibotti, B. C. Lin, M. C. Nason, O. Trofymenko, S. Telscher, S. H. Plummer, D. Wycuff, W. C. Adams, J. P. Pandey, A. McDermott, M. Roederer, A. N. Sukienik, S. O'Dell, J. G. Gall, B. Flach, T. L. Terry, M. Choe, W. Shi, X. Chen, F. Kaltovich, K. O. Saunders, J. A. Stein, N. A. Doria-Rose, R. M. Schwartz, A. B. Balazs, D. Baltimore, G. J. Nabel, R. A. Koup, B. S. Graham, J. E. Ledgerwood, J. R. Mascola; the VRC 603 Study Team, Safety and tolerability of AAV8 delivery of a broadly neutralizing antibody in adults living with HIV: A phase 1, dose-escalation trial. *Nat. Med.* **28**, 1022–1030 (2022).
40. J. P. Hughes, J. M. Baeten, J. R. Lingappa, A. S. Magaret, A. Wald, G. de Bruyn, J. Kiarie, M. Inambao, W. Kilembe, C. Farquhar, C. Celum; the Partners in Prevention HSV/HIV Transmission Study Team, Determinants of oer-coital-act HIV-1 infectivity among african HIV-1–serodiscordant couples. *J. Infect. Dis.* **205**, 358–365 (2012).
41. R. J. Shattock, J. P. Moore, Inhibiting sexual transmission of HIV-1 infection. *Nat. Rev. Microbiol.* **1**, 25–34 (2003).
42. M. A. Ramakrishnan, Determination of 50% endpoint titer using a simple formula. *World J. Virol.* **5**, 85–86 (2016).
43. E. Siebring-van Olst, C. Vermeulen, R. X. de Menezes, M. Howell, E. F. Smit, V. W. van Beusechem, Affordable luciferase reporter assay for cell-based high-throughput screening. *J. Biomol. Screen.* **18**, 453–461 (2013).
44. J. Haas, E. C. Park, B. Seed, Codon usage limitation in the expression of HIV-1 envelope glycoprotein. *Curr. Biol.* **6**, 315–324 (1996).
45. G. Mostoslavsky, A. J. Fabian, S. Rooney, F. W. Alt, R. C. Mulligan, Complete correction of murine Artemis immunodeficiency by lentiviral vector-mediated gene transfer. *Proc. Natl. Acad. Sci. U.S.A.* **103**, 16406–16411 (2006).

Acknowledgments: We wish to thank D. Lingwood and K. Clayton for many useful and insightful discussions. **Funding:** This work was supported by the Ruth L. Kirschstein Predoctoral Individual National Research Service Award 1F31AI131747-01A1 to J.M.B., NIGMS and NIAID R01AI131975 to H.N. and M.E.A., NIAID K22AI102769 to A.B.B., NIDA Avenir New Innovator Award DP2DA040254 to A.B.B., the MGH Transformative Scholars award to A.B.B., and funding from the Charles H. Hood Foundation to A.B.B. This independent research was supported by the Gilead Sciences Research Scholars Program in HIV to A.B.B. **Author contributions:** J.M.B., M.P., and A.B.B. designed the experiments. J.M.B., M.P., S.W.M., E.C.L.,

A.N., D.P., C.L.B., C.E.D., and W.F.G.-B. carried out experiments and analyzed data. H.N. and M.E.A. offered suggestions for experiments and provided materials. S.T. and V.D.V. provided humanized mice. J.M.B. and A.B.B. wrote the paper with contributions from all authors. **Competing interests:** A.B.B. is a named inventor on patent US9527904B2 held by the California Institute of Technology describing the vector used in this study. The other authors declare that they have no competing interests. **Data and materials availability:** All data associated with this study are present in the paper or the Supplementary Materials. This study did not generate sequence data or code. Plasmids generated in this study are available from A.B.B. under material transfer agreement with MGH. Purified FcγR proteins or their expression constructs are available from M.E.A. under material transfer agreement with Dartmouth College.

Submitted 4 January 2022
Resubmitted 13 April 2022
Accepted 31 May 2022
Published 27 July 2022
10.1126/scitranslmed.abn9662

Science Translational Medicine

Antibody-mediated prevention of vaginal HIV transmission is dictated by IgG subclass in humanized mice

Jacqueline M. BradyMeredith PhelpsScott W. MacDonaldEvan C. LamAdam NitidoDylan ParsonsChristine L. BoutrosCailin E. DealWilfredo F. Garcia-BeltranSerah TannoHarini NatarajanMargaret E. AckermanVladimir D. VrbanacAlejandro B. Balazs

Sci. Transl. Med., 14 (655), eabn9662. • DOI: 10.1126/scitranslmed.abn9662

Characterizing classes

Understanding the role of IgG subclasses in protecting against HIV infection is essential for developing the most effective antibody therapeutics. Here, Brady *et al.* tested the impact of changing IgG subclasses on protection conferred by the broadly neutralizing antibody, VRC07. VRC07 IgG2 exhibited reduced protection as compared to other IgG subclasses, whereas even low concentrations of VRC07 IgG1 conferred protection against vaginal challenge with HIV in humanized mice. These results suggest that, for some broadly neutralizing antibodies, IgG subclass considerably influences protection.